Accepted Manuscript

Transcutaneous implantation of valproic acid-encapsulated dissolving microneedles induces hair regrowth

Shayan Fakhraei Lahiji, Seol Hwa Seo, Suyong Kim, Manita Dangol, Jiyong Shim, Cheng Guo Li, Yonghao Ma, Chisong Lee, Geonwoo Kang, Huisuk Yang, Kang-Yell Choi, Hyungil Jung

PII: S0142-9612(18)30185-6

DOI: 10.1016/j.biomaterials.2018.03.019

Reference: JBMT 18545

To appear in: *Biomaterials*

Received Date: 16 December 2017

Revised Date: 1 March 2018

Accepted Date: 12 March 2018

Please cite this article as: Lahiji SF, Seo SH, Kim S, Dangol M, Shim J, Li CG, Ma Y, Lee C, Kang G, Yang H, Choi K-Y, Jung H, Transcutaneous implantation of valproic acid-encapsulated dissolving microneedles induces hair regrowth, *Biomaterials* (2018), doi: 10.1016/j.biomaterials.2018.03.019.

Transcutaneous Implantation of Valproic Acid-Encapsulated Dissolving Microneedles Induces Hair Regrowth

Shayan Fakhraei Lahiji[a], Seol Hwa Seo[b], Suyong Kim[a], Manita Dangol[a], Jiyong Shim[b], Cheng Guo Li[a], Yonghao Ma[a], Chisong Lee[a], Geonwoo Kang[a], Huisuk Yang[a], Kang-Yell Choi[b], Hyungil Jung[a,c,*]

[a] *Department of Biotechnology, Building 123, Yonsei University, 50 Yonsei-ro, Seodaemun-gu, Seoul 03722, Korea*

[b] *Translational Research Center for Protein Function Control, Building 117, Yonsei University, 50 Yonsei-ro, Seodaemun-gu, Seoul 03722, Korea*

[c] *Juvic Biotech, Inc., Building 102, Yonsei Engineering Research Park, 50 Yonsei-ro, Seodaemun-gu, Seoul 03722, Korea*

[*] Correspondence: Professor. Hyungil Jung, B513, Building 123, Yonsei University, 50 Yonsei-ro, Seodaemun-gu, Seoul 03722, Korea. Tel: +82-2-2123-2884, Fax: +82-2-362-7265

Email: hijung@yonsei.ac.kr (H. Jung)

Abstract

The interest in alternative material systems and delivery methods for treatment of androgenetic alopecia has been increasing in the recent decades. Topical application of valproic acid (VPA), an FDA-approved anticonvulsant drug, has been shown to effectively stimulate hair follicle (HF) regrowth by upregulating Wnt/β-catenin, a key pathway involved in initiation of HF development. Moreover, a majority of studies have suggested that cutaneous wound re-epithelialization is capable of inducing HF through Wnt/β-catenin pathway. Here, we report fabrication and evaluation of a novel VPA-encapsulating dissolving microneedle (DMN-VPA) that creates minimally invasive dermal micro-wounds upon application, significantly improving the VPA delivery efficiency. DMN-VPA not only delivers encapsulated VPA with higher accuracy than topical application, it also stimulates wound re-epithelialization signals involved in HF regrowth. Through a series of in vivo studies, we show that micro-wounding-mediated implantation of DMN-VPA upregulates expression of Wnt/β-catenin pathway, alkaline phosphatase, proliferating cell nuclear antigen, loricrin and HF stem cell markers, including keratin 15, and CD34 more effectively than topical application.

Keywords: valproic acid; dissolving microneedle; transdermal drug delivery; androgenetic alopecia; micro-wounding; hair regrowth

1. Introduction

Recently, numerous genetic and environmental factors determining the occurrence of androgenetic alopecia have been identified [1-3]. Despite considerable therapeutic advancements, current treating agents are limited by unsatisfactory cure rate, and potential adverse effects such as irritation, distant hypertrichosis [4,5], tachycardia [6-8], and sexual dysfunction in rare cases [9]. Recently, the well-known FDA-approved anticonvulsant drug, valproic acid (VPA), was shown to induce hair follicle (HF) regrowth [10-15], significantly more effectively than minoxidil [15-17]. VPA is among the carboxylic acid derivatives that activate several signaling pathways, including the Wnt/β-catenin pathway essentially involved in hair morphogenesis [15,18]. Remarkably, various studies highlight that β-catenin is highly expressed during the initial step of HF formation and growth [19-21], known as the anagen phase [22-24]. Although the exact mechanism underlying VPA function is not fully understood, several studies have suggested that VPA upregulates β-catenin expression by inhibiting glycogen synthase kinase 3β (GSK-3β) and promote HFs to transit from telogen (resting phase) to anagen (active phase) [25]. In addition, in the presence of Wnt, β-catenin levels are greatly increased, whereas in its absence, GSK 3β phosphorylates and destroys β-catenin proteins [26-29]. Consequently, we assume that the application of VPA results in (i) binding of Wnt protein with cell-surface receptors of the Frizzled family, (ii) inhibition of GSK-3β from phosphorylating β-catenin, and (iii) HF stem cell proliferation [30-32].

As for other therapeutic agents, precise dosing of VPA is crucial to prevent any adverse reactions [33,34]. Currently, the only available administration route for VPA to induce hair regrowth is topical delivery of solvent-based VPA (topical VPA) [12,17]. The solvent is employed as a chemical enhancer to facilitate the penetration of VPA across the skin barrier.

However, recent studies indicate that long-term administration of organic solvent-based therapeutics may irreversibly damage human health [35]. Moreover, the transdermal penetration rate varies greatly according to gender, race, and skin type [36], therefore, the achievement of accurate and efficient delivery of topical VPA was previously impractical. To address these limitations, dissolvable microneedles (DMNs) have been developed to deliver large molecules across the skin barrier [37]. DMNs can be used to encapsulate therapeutics and release them upon skin insertion in a minimally invasive manner [38]. However, as DMNs are solely fabricated over patches, their application onto the scalp and other hairy regions is impractical. Therefore, we hypothesized that patch-less implantation of solvent-free carboxymethyl cellulose (CMC) backbone-based VPA-encapsulating DMNs (DMN-VPA) would overcome the impediments of topical VPA as well as increase the VPA delivery efficiency across the skin. Utilizing CMC, a widely used FDA-approved biodegradable and biocompatible polymer for backbone matrix material of DMNs, provides the required mechanical strength for skin penetration and the ability to maintain activity of the encapsulated compounds post fabrication.

Additionally, a growing body of evidence suggests that β-catenin expression is upregulated during the proliferative phase of wound re-epithelialization, resulting in the development of embryonic HF epithelial cells [39-42]. Characterization of molecular events involved in HF regrowth unveiled the influence of wound re-epithelialization on HF neogenesis during the anagen phase [43,44]. Moreover, the number of studies focusing on wound-induced HF growth in both animal models [45] and humans [46] have increased over the last fifty years. Thus, we further hypothesized that implantation of DMNs, regardless of VPA encapsulation, amplifies epidermal Wnt/ β-catenin activation by creating microscopic pores (micro-wounds) in the skin.

Here, we set out to compare the efficiency of hair regrowth in mice upon application of topical VPA versus DMN-VPA. We demonstrate that implantation of DMN-VPA can be utilized as an effective approach to induce hair regrowth compared with topical VPA. Furthermore, through a series of *in vitro* and *in vivo* experiments, we systematically show that (i) DMN-VPA delivers the VPA with higher accuracy than topical VPA; (ii) regardless of VPA encapsulation, micro-wounding elevates Wnt signaling dependent proteins; and (iii) DMN-VPA exerts a dual-functionalized action by maximizing the VPA delivery efficacy while promoting HF regrowth via micro-wounding of the skin.

2. Materials and Methods

2.1. Animals

Male C3H mice (6 weeks old) were purchased from Orient Bio and given one week to adapt to the new environment. Then, a section of dorsal skin of the 7-week-old mice at telogen phase was gently shaved using a clipper, and treated with either topical control, topical VPA, DMN control, or DMN-VPA for 28 days (n = 7/group). Throughout the experiment, the mice were maintained under a 12-h light/dark cycle with food and water *ad libitum*. All procedures were performed in accordance with the guidelines and regulations of the experimentation ethics by Yonsei Laboratory Animal Research Center (YLARC), with approval from the International Animal Care and Use Committee (IACUC), Seoul, South Korea.

2.2. Topical Formulations and DMN Fabrication

Chemicals in all topical formulations were solubilised in a solvent containing ethanol, water, and propylene glycol (Sigma Aldrich) at a ratio of 5:3:2. Both topical VPA and DMN-

VPA arrays contained 50 µl of VPA (VPA dose/group: 1 M; Acros Organics). DMNs containing 12% CMC (90 kDa, Sigma Aldrich) polymer backbone were fabricated in four sets of 7 × 7 DMN-VPA arrays (total = 196 DMN-VPA per implantation) with 1.5 mm gap between each micro-cavity through centrifugal lithography fabrication method [48]. Briefly, the CMC-VPA solution was dispensed over micro-cavities at a rate of 0.6 kg.f/cm and 0.05 s/aliquot by using an automated X, Y and Z stage (SHOT mini 100-s, Musashi) and assembled vertically into a customized centrifuge rotor (Combi 514R, Hanil). Next, the drops were centrifuged at 2700 rpm for 2 min and solidified for 5 min at 4°C to fabricate DMN arrays with a height of 600 ± 22.32 µm. DMNs were implanted inside the skin using a micro-pillar-based system, as described previously [47].In addition, topical control and DMN control groups without VPA were included. All formulations and mixtures were homogenised and degassed simultaneously with a planetary centrifugal mixer (ARV-310; THINKY Corp.,). DMNs were fabricated and provided by Juvic incorporated.

2.3. Cell Viability and Cytotoxicity Analysis

Human dermal papilla cells (hDPCs) were purchased from Cell Applications Inc. and cultured in Dulbecco's modified Eagle's medium (DMEM). hDPCs were seeded in 24-well plates at a density of 4×10^4 cells per well and treated with either topical control, topical VPA, DMN control extract, or DMN-VPA extract for 72 h. Extracts from DMNs were obtained by dissolving the solidified DMNs in 1× PBS for 5 min at 23°C. Cell viability was assessed using CellTiter-Glo mixture, according to the manufacturer's instructions. Adenosine triphosphate was measured at 560 nm (BMG Labtech). Each value represents an average of five replicates and data are represented as relative activity compared with topical control.

The total number of apoptotic hDPCs upon each treatment was counted using FACS to evaluate biocompatibility of VPA. First, the cells were washed twice with PBS and once with Annexin V binding buffer (BD Biosciences). Then, the cells were stained for 15 min with Annexin V-FITC (BD Biosciences) followed by another 15 min with PI (BD Biosciences) at 4°C in the dark. Finally, flow cytometry was conducted on a FACSAria II system (BD Biosciences). The results were analysed using FACSDiva software.

2.4. Cutaneous Permeation Analysis

Diffusion of topical formulations and DMNs through isolated pig cadaver skin was compared using a customised Franz diffusion chamber (SES GmbH) equipped with a temperature control system to maintain skin humidity. The diffusion chamber, set at 32 ± 1°C, was magnetically stirred at 250 rpm to mimic blood circulation and to maintain temperature throughout the experiment. First, diffusion of 50 µl (0.1% w/w) rhodamine B (479 Da, Sigma Aldrich) in the form topical rhodamine and DMN-rhodamine was visualised over the epidermis layer of pig cadaver skin (surface area: 2.5 cm^2, thickness: 1 mm; CRONEX) for 90 min. Images were taken every 30 min using an M165 FC bright-field optical microscope (Leica). The skin was gently wiped to completely remove excess rhodamine before each recording.

Dissolution kinetics of 1 M VPA in the form of topical VPA and DMN-VPA across pig cadaver skin was evaluated by taking samples from the chamber every 10 min up to 1 h and every 60 min up to 3 h. The skin was next soaked inside the chamber for 1 h and the amount of VPA detected at 4 h was set as 100%. Topical formulation and DMN without VPA were used as controls.

Additionally, diffusion of 50 µl (0.1% w/w) FITC (Sigma Aldrich) in topical and DMN-encapsulated forms was captured and measured using an *in vivo* imaging system (Spectral Lago X; Spectral Instruments Imaging) at 30, 60, and 90 min for 5 s with an excitation wavelength of 445–490 nm and an emission wavelength of 515–575 nm. All data were analysed and expressed using AMIView software.

2.5. Histological and Immunohistochemical Analysis

Skin tissues were excised from the shaved dorsal area, fixed overnight in 4% (w/v) paraformaldehyde (Sigma Aldrich), dehydrated, and paraffinised (Paraplast; Leica). The tissues were then sliced into 4-µm sections, deparaffinised using three changes of xylene (Sigma Aldrich), and rehydrated by passage through a series of decreasing graded ethanol concentrations. The sections were stained with hematoxylin for 5 min and with eosin for 1 min (H&E staining) and photographed using a M165 FC microscope (Leica).

For antigen retrieval, fresh tissue sections were autoclaved in 10 mM sodium citrate buffer, pre-incubated in PBS, and blocked in PBS containing 10% bovine serum albumin at 23°C for 30 min. Then, the sections were incubated overnight at 4°C with primary antibodies targeting the following proteins: β-catenin (1:100; BD Biosciences), PCNA (1:500; Santa Cruz Biotechnology), loricrin (1:500; Covance), K14 (1:500; Covance), K15 (1:200; Thermo Scientific), and CD34 (1:30; Abcam). After incubation, the sections were rinsed with PBS and incubated with 1:400 diluted Alexa Fluor 488- and Alexa Fluor 555-conjugated IgG secondary antibodies (Molecular Probes) at 23°C for 1 h and counterstained with 4′,6-diamidino-2-phenylindole (DAPI, 1:5000; Boehringer Ingelheim). The fluorescent signals were visualised

using an LSM510 META confocal microscope (Carl Zeiss) and the mean intensity of each group was measured using ZEN imaging software (Carl Zeiss).

For ALP staining, tissues were fixed in 4% paraformaldehyde overnight and embedded in Tissue Tek O.C.T. compound (Sakura FineTechnical). Cryosections of 10 μm were rinsed in TN buffer (0.1 M Tris-HCl, pH 9.5; 0.1 M NaCl), incubated in 120 mg/ml 4-nitroblue tetrazolium (Sigma Aldrich) followed by 60 mg/ml BCIP (5-bromo-4-chloro-3-indolylphophate, Sigma Aldrich) in TN buffer for 30 min, and analysed as above.

2.6. Western Blot Analysis

Tissues from shaved dorsal regions of each group were ground and lysed in radioimmunoprecipitation assay buffer (150 mM NaCl, 10 mM Tris, pH 7.2, 0.1% sodium dodecyl sulphate (SDS), 1.0% Triton X-100, 1% sodium deoxycholate, 5 mM ethylenediaminetetraacetic acid). Next, equal amounts of protein were separated on 12% SDS polyacrylamide gels and transferred onto PROTRAN nitrocellulose membranes (Schleicher and Schuell Co.). After blocking for 1 h with PBS containing 5% non-fat dry skim milk, the membranes were incubated with antibodies specific for β-catenin (1:1000; Santa Cruz Biotechnology), PCNA (1:500, Santa Cruz Biotechnology), loricrin (1:1000; Covance), K14 (1:1000; Covance), K15 (1:1000; Thermo Scientific), CD34 (1:1000; Abcam), and ALP (1:100; Abcam) at 4°C overnight. The membranes were washed three times and incubated with horseradish peroxidase-conjugated anti-rabbit (1:5000; Bio-Rad Laboratories) and anti-mouse (1:5000; Cell Signaling Technology) IgG secondary antibodies. Finally, the immunoreactive bands were visualised with enhanced chemiluminescence (Amersham Bioscience) using the LAS-3000 luminescent image analyser and quantified with Science Lab 2005 (Fujifilm).

2.7. qRT-PCR

Total RNA was extracted with TRIzol reagent (Invitrogen) and reverse-transcribed to cDNA using M-MLV reverse transcriptase (Invitrogen) for use in RT-PCR. GAPDH was employed as an endogenous control for quantitation using the comparative cycle-threshold method. qRT-PCR was carried out on a System 2700 (Applied Biosystems) using the following thermal program: 94°C for 5 min, followed by 30 cycles of 94°C for 30 s, 60°C for 1 min, and 72°C for 1 min. The following primer sets were used: ALP, forward 5′-CAGGTCCCACAAGCCCGCAA-3′ and reverse 5′-CCCGGTGGTGGGCCACAAAA-3′; PCNA, forward 5′-GCCATGGGCGTGAACCTCACCA-3’ and reverse 5′-TACACAGCTGTACTCCTGTTCTGG-3′; loricrin, forward 5′-CCTACCTGGCCGTGCAAG-3′ and reverse 5′-CATGAGAAAGTTAAGCCCATCG-3′; K14, forward 5′-GGACGCCCACCTTTCATCTTC-3′ and reverse 5′-ATCTGGCGGTTGGTGGAGG-3′; K15, forward 5′-AGCTATTGCAGAGAAAAACCGT-3′ and reverse 5′-GGTCCGTCTCAGGTCTGTG-3′; CD34, forward 5′-CTTTCAACCACTAGCACTAGCC-3′ and reverse 5′-TGCCCTGAGTCAATTTCACTTC-3′.

2.8. Statistical Analysis

Means were compared using Student’s *t*-test, or one-way or two-way analysis of variance (ANOVA) using GraphPad Prism 6 software (GraphPad Software Inc.). *P*-values of < 0.05 were considered significant.

3. Results

To test the hypothesis that DMN-VPA promotes anagen onset and elevates expression of HF related proteins while stimulating wound-associated signals (Fig. 1a), we investigated skin permeation efficiency of VPA and micro-wounding effects on HF regrowth. DMNs with a height of 600 ± 22.32 μm and a tip diameter of 20 ± 8 μm were fabricated over 7 × 7 micro-cavities through centrifugal lithography fabrication method, and inserted into the skin using a patch-less, custom-made, micro-pillar-based implantation system (Fig. 1b & c, Supplementary Fig. 1).

3.1. Transcutaneous Permeation Measurement

The transcutaneous permeation efficiency of the same amount of model dye in the form of topical solution and DMN formulation was compared through a set of *in vitro* and *in vivo* experiments using rhodamine and fluorescein isothiocyanate (FITC) dyes. First, we examined the diffusion characteristics of topical rhodamine and DMN-encapsulated rhodamine (DMN-rhodamine) for 90 min using a customized diffusion cell apparatus (Fig. 1d). This system was customized to isolate the skin and minimize skin water loss through the use of a receptor chamber set at 32 ± 1°C to mimic the actual biological environment of human skin. At each recording interval, excess rhodamine was gently washed from the skin surface to accurately detect the amount that had permeated. At 30 min post application, the signal intensity produced by DMN-rhodamine, visible as an array of spots, was remarkably higher than that produced by topical rhodamine. At 60 min, the strong DMN-rhodamine signal had further diffused outside each spot, whereas the topical rhodamine had only slightly increased in intensity. At 90 min, the intensity of the topical rhodamine had increased; however, the rhodamine signal was incomparably stronger in DMN-rhodamine-treated skin. These findings suggest that application

of DMN-rhodamine delivers rhodamine with higher accuracy and efficiency than topical application.

Additionally, the cutaneous penetration of DMN was evaluated by *in vivo* imaging upon administration of either topical or DMN-encapsulated FITC (DMN-FITC). As shown in Fig. 1e, the FITC intensity in both groups continuously increased up to 90 min; however, the overall signal intensity generated by DMN-FITC was notably higher than that produced by topical FITC. These results confirmed the superior permeation efficiency of DMN.

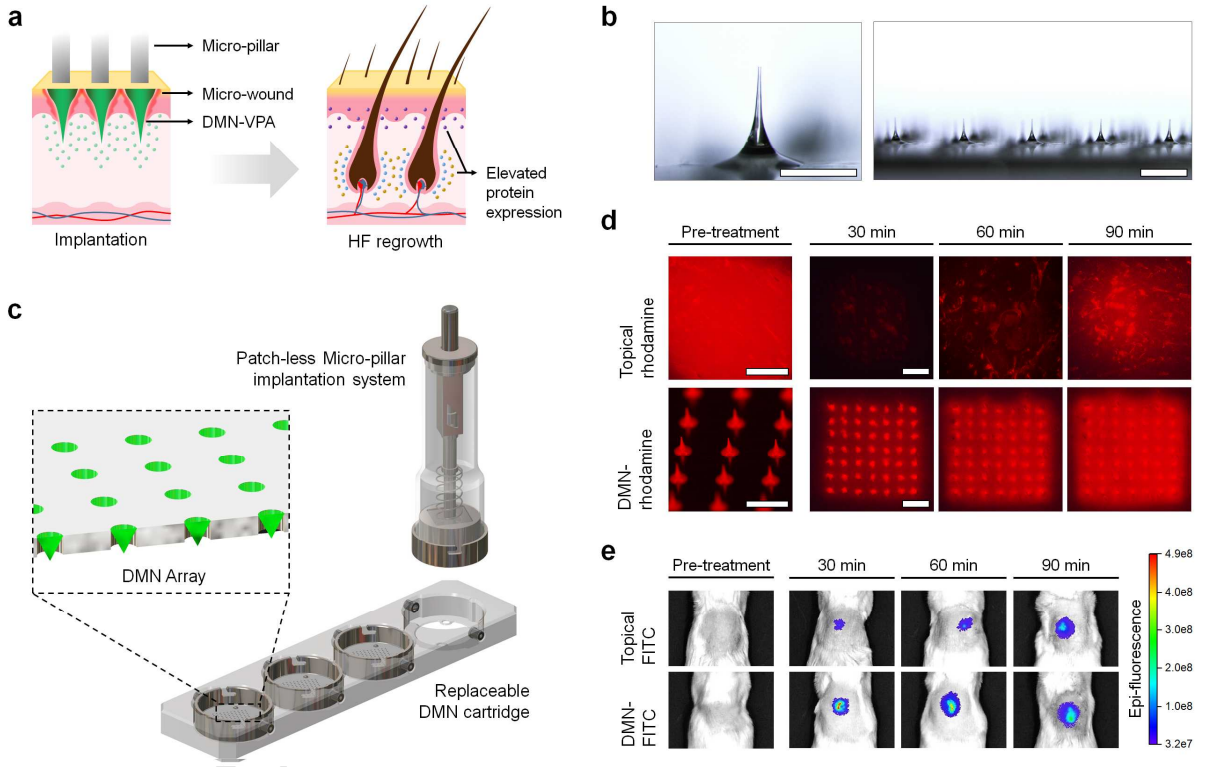

Fig. 1. Transcutaneous DMN implantation promotes delivery efficiency as compared to topical application. a, Schematic representation of DMN-VPA implantation. b, Microscopic photographs of CMC backbone-based DMNs. DMNs were fabricated in 7 × 7 arrays with an overall height of 600 ± 22.32 μm and a tip diameter of 20 ± 8 μm. Scale bars are 500 μm (left) and 1 mm (right). c, Illustration of the patch-less implantation and delivery systems. DMN arrays were fabricated over micro-cavities and applied using a micro-pillar application system. d, DMN encapsulation

enhances rhodamine delivery inside pig cadaver skin. At 90 min post application, most of the topical rhodamine was washed out from the skin surface, whereas DMN-rhodamine produced a notably sharp intensity outside the implanted spots. Scale bars correspond to 1.5 mm (pre-treatment) and 3 mm (right panels). e, DMN encapsulation enhances FITC delivery in vivo. Similar to the results obtained with rhodamine, DMN-FITC implantation showed higher skin permeability efficiency than topical FITC.

3.2. Activity and biocompatibility *of VPA*

As VPA is a well-known activator of Wnt signaling pathway [18], we measured the activity of VPA based on its capability in activating Wnt receptor cells upon treatment with topical VPA and DMN-VPA extracts. Both VPA treatments stimulated the activity to a level similar to that induced by fresh VPA prepared in distilled water (Fig. 2a). These results suggest that there is no significant activity loss during VPA encapsulation or topical VPA formulation.

Next, we assessed the biocompatibility of VPA using fluorescence-activated cell sorting (FACS) of hDPCs based on annexin V and propidium iodide (PI) staining (Supplementary Fig. 2), which allows the identification of viable cells (–/–), early apoptotic cells (+/–), and late apoptotic cells (+/+) (Fig. 2b). Topical control, topical VPA, DMN control, and DMN-VPA treatments maintained 91.3%, 86.2%, 91.3%, and 85.2% of viable cells, respectively. Moreover, there was no difference in the percentage of apoptotic cells among hDPCs treated with topical VPA (1.8%) and DMN-VPA (1.8%); therefore, we conclude that the dosage of 1 M VPA is biocompatible.

3.3. Skin Penetration Evaluation of Topical VPA and DMN-VPA

The permeation of topical VPA and DMN-VPA was evaluated using the diffusion cell apparatus. To evaluate the permeation rate of 1 M VPA, we applied topical VPA and DMN-VPA

on pig cadaver skin and quantified the amount of VPA delivered into the receptor chamber by sampling every 10 min for 60 min and every 30 min for 120 min for each treatment. Plotting of the cumulative VPA release revealed that DMN-VPA induced faster as well as higher accumulation in the chamber than topical VPA (Fig. 2c). At 120 min post application, the total amount of VPA delivered by DMN-VPA and topical VPA was 87 ± 12.1% and 21 ± 13.6%, respectively. VPA was not detected in receptor chambers of skins treated by topical and DMN control. These findings indicate that DMN-VPA accurately delivers encapsulated VPA with significantly higher efficiency than topical VPA.

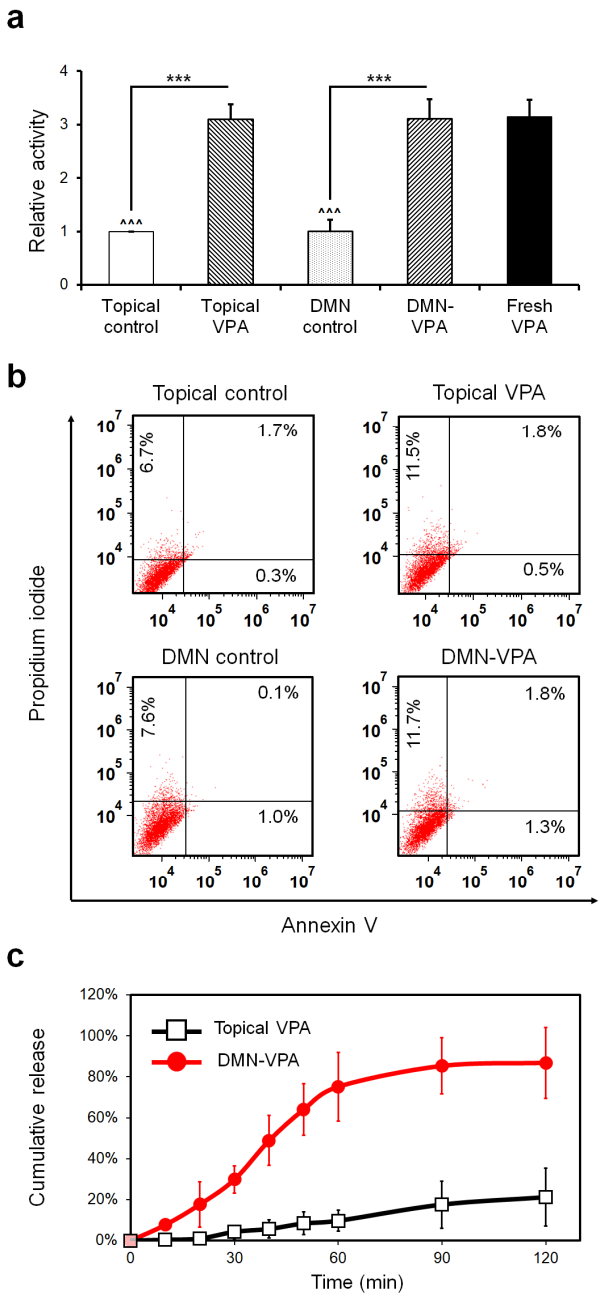

Fig. 2. VPA retains activity and biocompatibility in topical as well as DMN-encapsulated form. a, Both topical VPA and extract of DMN-VPA (1 M VPA per group) significantly increased activity of Wnt receptor cells by 3-fold, up to the level induced by fresh VPA, with no significant differences between the VPA treatment groups. Data are expressed as mean ± s.e.m (n = 5). ^^^P

< 0.001 vs. fresh VPA, ***P < 0.001. b, FACS results indicate that VPA does not stimulate hDPC apoptosis. c, DMN-VPA accurately delivers VPA at a faster rate, than topical VPA. At 120 min post application, the total amount of VPA delivered into the receptor chamber by DMN-VPA was 87 ± 12.1% whereas topical VPA delivered only 21 ± 13.6% of loaded VPA. Data are shown as mean ± s.d. (n = 6).

3.4. Hair Regrowth Evaluation

To evaluate the efficacy of DMN-VPA in inducing hair regrowth, we shaved the dorsal skin area of 7-week-old male mice at telogen phase and applied 50 µl of 1 M VPA either as topical VPA or as DMN-VPA once a day for 28 days (n = 7/group). To confirm whether hair regrowth was induced solely by application of VPA in these treatment groups, we included two control groups of mice treated daily with either topical control or DMN control (n = 7/group). At day 28, all mice of the DMN-VPA-treated group and two out of seven mice treated with topical VPA, showed hair regrowth (Fig. 3a). The regrown hairs uniformly covered the entire shaved region in DMN-VPA-treated mice. In contrast, in the topical VPA group, hair regrowth was mainly concentrated in the center of the shaved region (indicated by a dashed line in Fig. 3a). In both the control groups, none of the mice showed hair regrowth. These findings show that DMN-VPA delivers encapsulated VPA with a high accuracy over the whole region.

The effect of VPA on hair density was evaluated by quantifying the number of hair shafts/cm^2 over an untreated (unshaved) region in comparison to the treated (shaved) region for each mouse to account for natural variation in hair density (n = 2/group). In topical VPA-treated mice, the shaft density was 634.5 ± 9.1 shafts/cm^2 in the untreated region and 642 ± 15.5 shafts/cm^2 in the treated area, a mean difference of 7.5 ± 6.3 shafts/cm^2 (Fig. 3b). In the DMN-

VPA group, hair shaft density differed by 35 ± 19.8 shafts/cm^2, being 648.5 ± 13.44 shafts/cm^2 to 683.5 ± 6.3 shafts/cm^2 in unshaved and shaved regions, respectively (Fig. 3c). Next, we compared regrown hair shaft thickness of the same type in topical VPA- and DMN-VPA-treated mice (n = 20/group). In both groups, hair shaft thickness varied widely, from 7.26 μm to 51.64 μm (Supplementary Fig. 3). However, the mean hair shaft thickness under topical VPA (19.05 ± 11.41 μm) was significantly lower than that under DMN-VPA treatment (27.15 ± 12.01 μm) (Fig. 3d). Control groups were excluded from the comparison due to the lack of hair regrowth at 28 days post experiment. Scanning electron microscopy (SEM) revealed no damage to the surface of regrown hair shafts in both treatment groups (Fig. 3e).

Additionally, we sectioned the treated dorsal skin regions to compare the hair regrowth characteristics in more detail (Fig. 3f). The mice treated with DMN-VPA had the highest number of HFs among the four groups, followed by topical VPA. Histomorphometrical analysis of HFs showed that DMN-VPA treatment also promoted telogen-to-anagen transition more effectively than topical VPA (Fig. 3g). As expected, most of the HFs in both control groups remained in telogen phase at day 28. To verify that the normal epidermis properties was not damaged by DMN-VPA application, the epidermal thickness was measured for each group. The epidermis was 13.81 ± 1 μm thick on average (n = 10/group), with no significant differences between and within groups (Fig. 3h). However, due to the difference in the number of HFs in each group, the dermal thickness significantly differed (n = 10/group). The dermal thickness in the topical control group was 417.3 ± 20 μm, and it significantly increased to 563 ± 135 μm upon treatment with topical VPA. Likewise, DMN-VPA treatment significantly increased the mean dermal thickness from 505 ± 27 μm to 661 ± 103 μm (Fig. 3i). Also, the dermal thickness under DMN-VPA treatment was significantly higher than that upon topical VPA application. Altogether,

these data imply that DMN-VPA effectively elevates HF regrowth by accelerating telogen-to-anagen transition without damaging the hair shafts or epidermis layer.

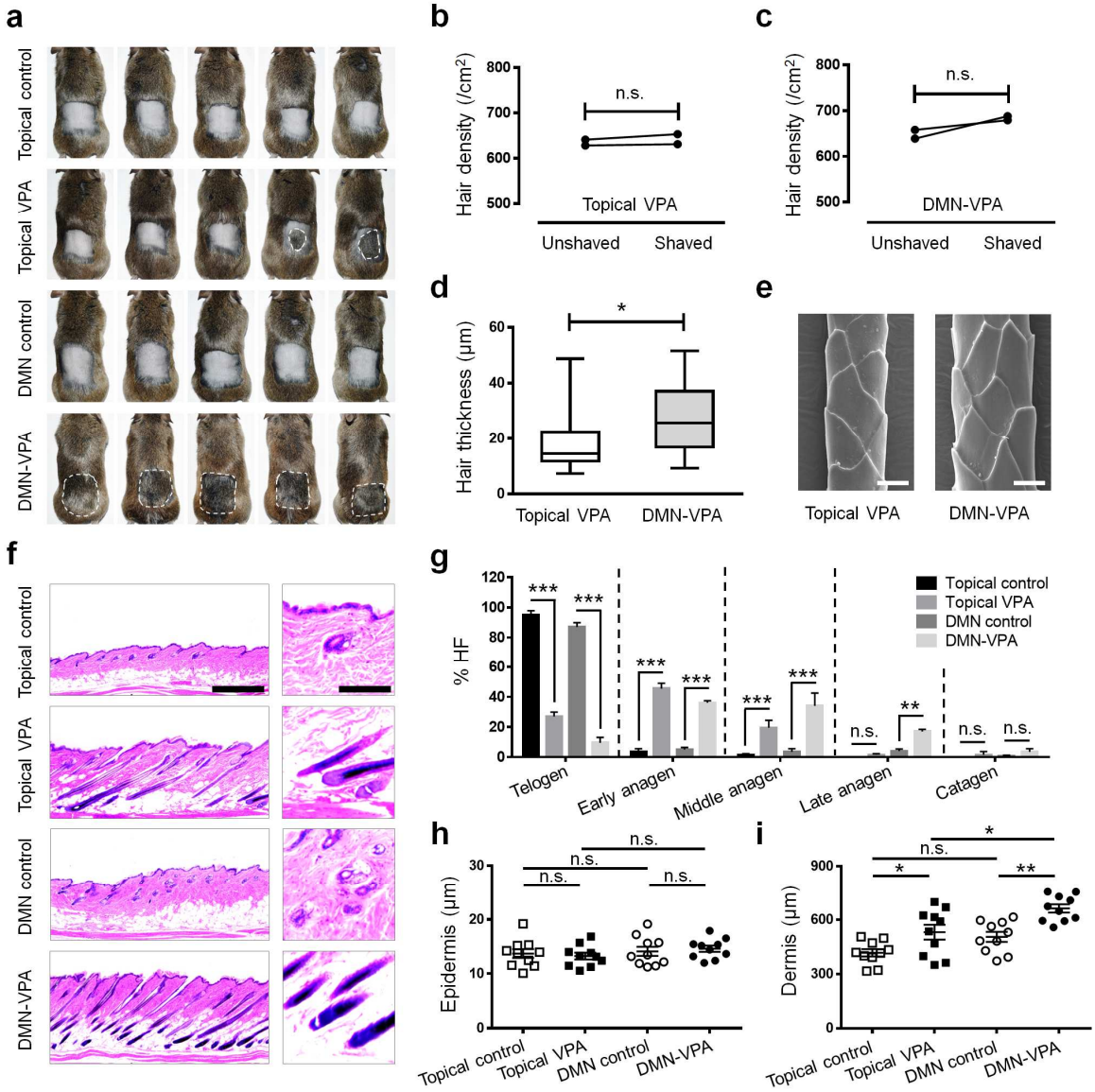

Fig. 3. DMN-VPA induces hair regrowth more effectively than topical VPA. a, DMN-VPA implantation induces complete hair regrowth. At day 28, all mice in the DMN-VPA-treated group had fully grown hair shafts, whereas hair regrowth was observed in only two out of seven mice treated with topical VPA. Mice in both topical control and DMN control groups did not exhibit any hair regrowth. Dashed lines highlight regions of hair regrowth within the shaved

areas. b & c, VPA enhances hair shaft density. Hair shaft density was 7.5 ± 6.3 shafts/cm^2 and 35 ± 19.8 shafts/cm^2 higher in topical VPA- and DMN-VPA-treated regions than in untreated (unshaved) regions, respectively. d, DMN-VPA implantation increases hair shaft thickness. The thickness of DMN-VPA-induced hair shafts (27.15 ± 12.01 μm) was significantly higher than that induced by topical VPA (19.5 ± 11.41 μm). Data are expressed as mean ± s.e.m with min-to-max whiskers (n = 20). e, VPA-stimulated anagen onset does not affect the quality of regrown cuticle scales. Bars represent 10 μm. f, Application of DMN-VPA induces hair regrowth with a high efficacy. DMN-VPA induced the highest density of HFs, followed by topical VPA (left). Skin sections of HF regions at a magnification of 5× (right). Bars represent 500 μm (left) and 100 μm (right). g, DMN-VPA enhances telogen-to-anagen transition. h, Implantation of DMN-VPA does not affect epidermal thickness. i, Dermal thickness increases upon VPA treatment. The dermal thickness in the topical control group was the lowest (417 ± 98 μm), followed by DMN control (505 ± 27 μm), topical VPA (563 ± 135 μm), and DMN-VPA (661 ± 103 μm). Data are expressed as mean ± s.e.m in g, h and i (n = 10). *P < 0.05 and **P < 0.01.

3.5. Assessment of Epidermal Marker Expression

To confirm effects of DMN-VPA on HF regrowth, we conducted immunohistochemical analysis of β-catenin, PCNA, loricrin, and keratin 14 (K14) in the tissues from the shaved region (Fig. 4a; for images without DAPI refer to Supplementary Fig. 4). Quantitative analysis of immunohistochemical staining showed that DMN-VPA induced the highest expression level of β-catenin, an essential protein of HF morphogenesis and hair cell proliferation in both epidermis and HF regions [20], at 2.435 ± 0.215, followed by topical VPA (1.642 ± 0.168; Fig. 4b, top left). In contrast, the expression of β-catenin in DMN control (1.377 ± 0.174) was higher than that in topical control (0.954 ± 0.119). PCNA, a cell proliferation marker [17], was highly expressed in all experimental groups, except the topical control group (Fig. 4b, top right). The expression intensity of PCNA in the DMN-VPA-treated group was the highest, at 2.177 ± 0.215. Interestingly, the expression in the DMN control group (1.932 ± 0.176) was higher than that in

both topical VPA (1.870 ± 0.202) and topical control (0.987 ± 0.099)-treated groups. Additionally, loricrin, a terminally differentiated hair marker expressed in epidermal cells [49], was highly upregulated upon application of DMN-VPA (2.685 ± 0.176) and DMN control (2.190 ± 0.182; Fig. 4b, bottom left). As seen with PCNA, DMN control caused a significant increase in loricrin expression as compared to topical control (1.086 ± 0.168). Finally, the expression of K14, an epidermal cell shape maintenance marker [50], was quantified to evaluate the effects of VPA implantation on epidermal structure. K14 expression was increased in both topical VPA (2.363 ± 0.141) and DMN-VPA (2.578 ± 0.194)-treated groups as compared to topical control (1.813 ± 0.145) and DMN control (2.104 ± 0.160) (Fig. 4b, bottom right).

Consistent with immunohistochemical results, western blot analysis revealed that protein expression level of β-catenin, PCNA, loricrin and K14 in topical VPA-, DMN control-, and DMN-VPA-treated groups was increased (Fig. 4c). Quantitative analysis showed that all three proteins were significantly higher expressed in VPA-treated than in control groups. In addition, the DMN control also induced remarkably higher expression of all markers than the topical control. Interestingly, expression levels of loricrin and K14 did not significantly differ between the topical VPA-treated and DMN control groups (Fig. 4d). K14 protein level was not upregulated in both VPA groups, with respect to the control-treated groups.

To evaluate mRNA expression levels of PCNA, loricrin, and K14, we performed quantitative reverse transcription (qRT-)PCR of the treated skin tissues. The relative gene expression levels of PCNA and K14 were significantly increased following VPA treatment. Moreover, in the DMN control group, PCNA expression was slightly lower but not significantly different from those in the topical VPA group (Fig. 4e). Loricrin expression in topical VPA was significantly upregulated, whereas both DMN-treated groups showed highly elevated mRNA

expression levels. Overall, mRNA level of markers was significantly higher in DMN-VPA than in topical VPA, and higher in DMN control than in topical control groups without any significant differences in between topical VPA- and DMN control-treated groups.

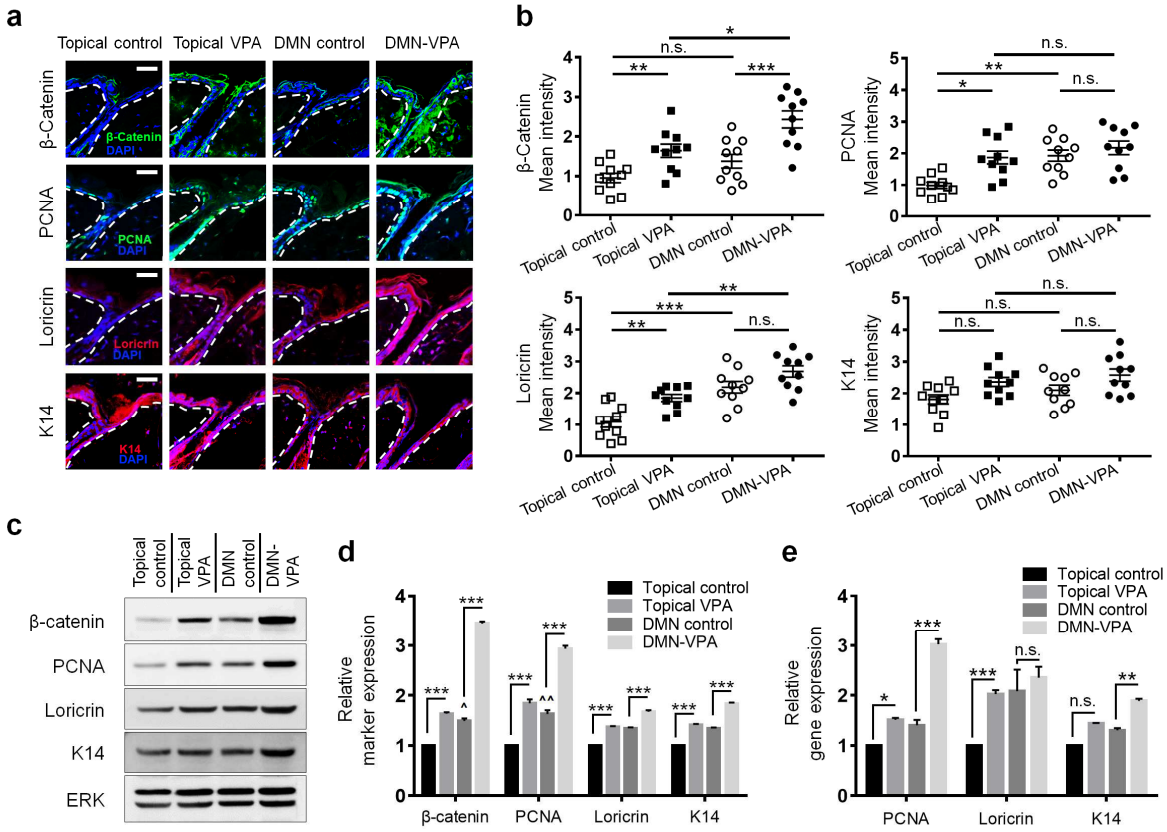

Fig. 4. DMN-VPA upregulates epidermal protein expression. a, Protein expression of β-catenin, PCNA, loricrin, and K14 is upregulated in both VPA-treated groups and DMN control as compared to the topical control. Bars represent 10 μm for all panels. b, Implantation of DMN-VPA significantly increases β-catenin, PCNA, and loricrin expression. c, Implantation of DMN-VPA upregulates epidermal proteins. DMN-VPA induced peak expression levels of all examined epidermal markers followed by topical VPA. d, Both VPA treatment and DMN implantation significantly increase expression of epidermal proteins in tissues. DMN control remarkably increased epidermal marker expression as compared to the topical control. e, DMN-VPA implantation increases gene expression of epidermal proteins. The DMN-VPA-treated group showed the highest gene expression levels for all markers. There were no significant differences

in gene expression levels between topical VPA and DMN control. Data in b (n = 10), d, and e (n = 3) are the mean ± s.e.m. *P < 0.05, **P < 0.01, and ***P < 0.001; ^P < 0.05 and ^^P < 0.01 vs. topical VPA.

3.6. Evaluation of HF Marker Expression

Next, we examined expression levels of β-catenin, keratin 15 (K15), and CD34, which are among the essential HF markers known to increase in expression during hair growth, by immunohistochemical staining (Fig. 5a; for images without DAPI refer to Supplementary Fig. 5). Expression of β-catenin, keratin 15 (K15), and CD34 was remarkably increased at the lower bulge and hair germ of VPA-treated groups. Quantitative analyses of immunohistochemical staining indicated that β-catenin expression was significantly increased in both VPA-treated groups, with relative intensities of 1.432 ± 0.211 for topical VPA and 2.176 ± 0.1921 for DMN-VPA (Fig. 5b, top). Moreover, the β-catenin level in DMN control (0.952 ± 0.147) was higher but not significantly different from that in topical control (0.617 ± 0.120). Likewise, VPA treatment caused a significant increase in K15 expression, a stem cell marker of HF [51], in both topical VPA (1.578 ± 0.156) and DMN-VPA (2.306 ± 0.202)-treated groups. Interestingly, K15 showed significantly higher expression in DMN control (1.118 ± 0.169) than in topical control (0.229 ± 0.148, Fig. 5b, middle). Expression of CD34, a glycoprotein expressed in the HF [51], was the highest following DMN-VPA (2.219 ± 0.147) treatment, followed by topical VPA (1.686 ± 0.133) treatment. DMN control-treated mice (1.058 ± 0.117) also exhibited CD34 higher expression than topical control animals (0.712 ± 0.136, Fig. 5b, bottom). The quantitative analysis of immunohistochemical staining revealed that, in addition to DMN-VPA, implantation of DMN control also effectively enhanced growth-related protein expression in dermal papilla.

Furthermore, expression of alkaline phosphatase (ALP), a prominent dermal papilla marker expressed in the HF of dermal papilla [52], was analyzed to confirm HF regrowth. We discovered that ALP expression was increased not only in VPA-treated groups, but also in the DMN control group (Fig. 5c).

Western blot analysis showed high protein expression levels of K15, CD34, and ALP in both the VPA-treated groups as well as in the DMN control tissues (Fig. 5d). Interestingly, DMN control was able to increase the expression of K15 and CD34 to the same levels as topical VPA (Fig. 5e). In addition, expression of ALP was also significantly higher in DMN control- than in topical control-treated mice.

Finally, gene expression of K15, CD34 and ALP was analyzed using qRT-PCR. The highest mRNA levels of the selected markers were detected in the DMN-VPA-treated followed by topical VPA- and DMN control-treated groups (Fig. 5f). Nevertheless, the expression levels of markers were remarkably increased following DMN control as compared to topical control treatment. Altogether, these findings suggest that implantation of dual-functionalized DMN-VPA promotes expression of β-catenin, HF stem cell markers and ALP significantly more effectively than topical VPA.

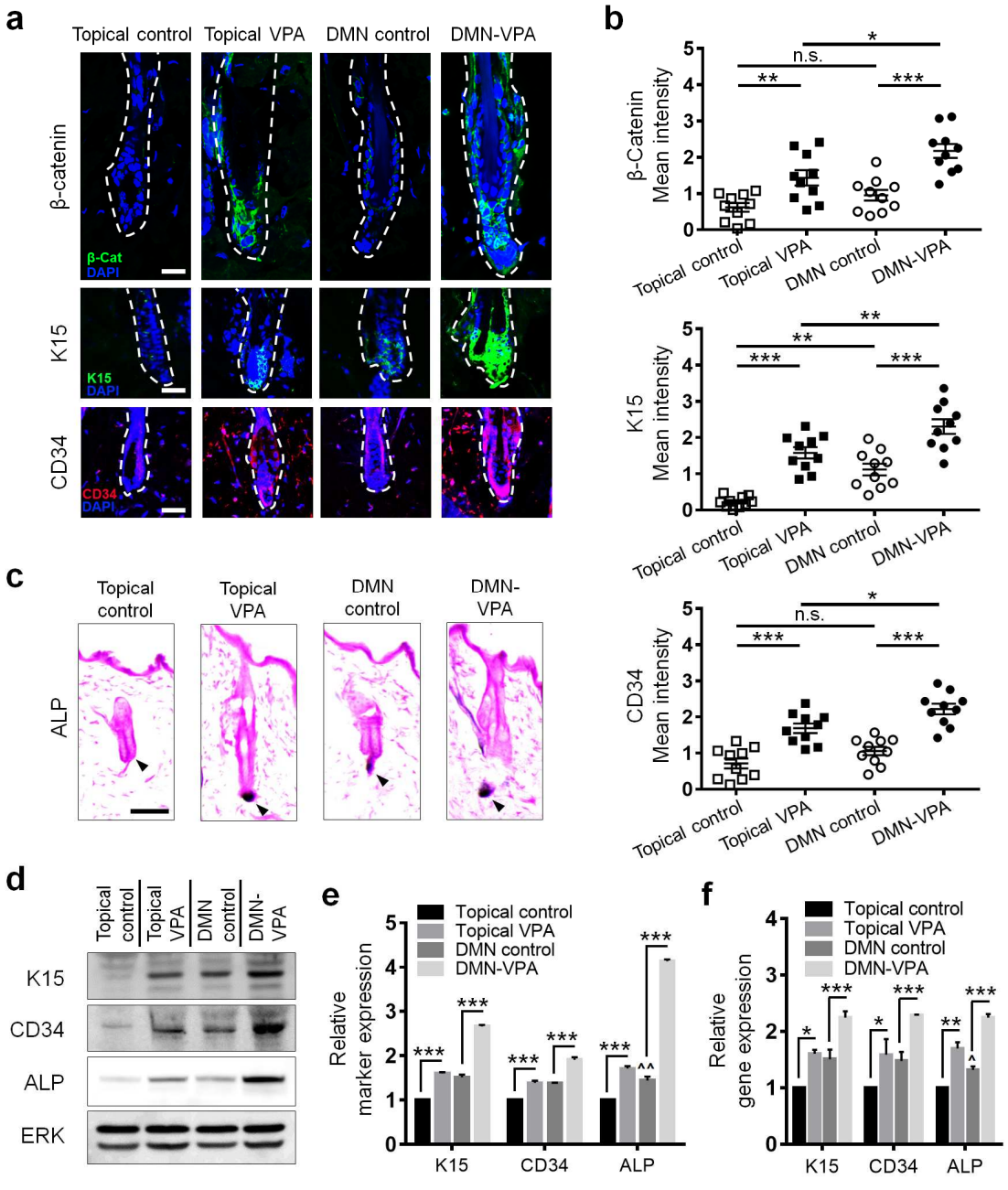

Figure 5. Implantation of DMN-VPA upregulates β-catenin, K15, CD34 and ALP expression levels. a, VPA treatment significantly increases protein and stem cell expression levels at the lower bulge and hair germ. Bars represent 10 μm for all panels. b, DMN-VPA elevates β-catenin, K15, and CD34 expression more effectively than topical VPA. Also, the DMN control more strongly induces HF stem cell protein expression than the topical control. c, VPA treatment and

DMN control induce ALP expression. Bars represent 50 μm for all panels. d, DMN-VPA implantation strongly elevates HF stem cell-related protein expression. Western blot analysis of K15, CD34, and ALP reveals that DMN-VPA treatment results in the highest expression levels, followed by topical VPA. e, DMN control effectively elevates K15 and CD34 protein levels. f, Gene expression level of HF markers is the highest in mice treated with DMN-VPA, followed by topical VPA and DMN control. Data in b (n = 10), e, and f (n = 3) are expressed as the mean ± s.e.m. *P < 0.05, **P < 0.01, and ***P < 0.001. ^P < 0.05, ^^P < 0.01 for DMN control as compared with topical VPA.

4. Discussion

In this study, we developed a dual-functionalized DMN-VPA for transcutaneous delivery of VPA that not only enhanced the drug penetration efficiency, but also stimulated HF stem cells by creating micro-wounds in the skin. Although the action mechanism of VPA is not yet fully known, the vast majority of studies suggest that VPA inhibits GSK 3β from phosphorylating β-catenin, a protein essential for HF morphogenesis [39]. Additionally, evidence suggests that in the absence of β-catenin, stem cells differentiate into epidermal rather than hair keratinocytes. Therefore, in addition to the therapeutics currently available on the market, VPA is a high-potential candidate for the treatment of androgenetic alopecia in future.

DMN-VPA was fabricated using centrifugal lithography, a recently developed single-step polymer shape forming and solidification combined method by which the activity of encapsulated compounds is shown to be highly maintained throughout the fabrication process [53]. Our study showed that DMN-VPA has a significantly higher penetration capability and diffuses at a remarkably faster rate than the topical VPA formulation. This is likely owing to the different VPA application and release sites: topical VPA solution is applied onto the skin surface,

and only a small quantity can effectively permeate through the skin pores, whereas DMN-VPA is implanted below the epidermis layer and directly delivers VPA inside the skin.

By evaluating expression levels of β-catenin protein that accounts for both epidermis and HF activity, epidermal specific proteins including PCNA, loricrin, K14, HF specific stem cells including K15, CD34, and ALP, we demonstrated that implantation of DMN-VPA promotes hair regrowth and accelerates telogen-to-anagen transition more effectively than a solvent-based topical VPA formulation. As vast majority of studies suggested, the accelerated transition observed in DMN-VPA-treated mice is due to increased expression of Wnt/β-catenin pathway [22,54]. Moreover, both western blotting and gene expression analysis revealed substantially higher epidermal and HF papilla-related protein expression in mice that had received DMN-VPA. On the basis of these findings, we conclude that effectivity of DMN-VPA in inducing epidermal proteins, HF stem cells, ALP and Wnt/β-catenin pathway is remarkably higher topical VPA.

In addition, our findings showed that micro-wounding upregulates HF-inducing proteins in a minimally invasive manner, obliterating the need for creating large and painful wounds. To our knowledge, this has not been previously reported. Although hair regrowth was not observed in DMN control-treated mice, quantitative immunohistochemistry revealed higher protein expression of β-catenin, PCNA, loricrin, K15, and CD34 in DMN control than in topical control animals. Moreover, no abnormal properties was observed in the epidermis cell layers of mice treated with DMNs. Both western blot analysis and qRT-PCR revealed high expression levels of loricrin, K14, K15, and CD34 upon treatment with either topical VPA or DMN control. These results, together with previous findings on the correlation between wound re-epithelisation and enhanced hair growth [42,55], confirm our hypothesis on the potential of micro-wounding in upregulating hair regrowth. However, additional studies should address the molecular

mechanisms involved in wound-induced re-epithelisation and the potential of micro-wounding in inducing hair regrowth.

In vivo hair growth analysis in mice demonstrated that DMN-VPA induced a higher hair shaft density than topical VPA. Although further investigations are required, based on these and the above-mentioned facts, we assume both micro-wounding and improved VPA permeation to be accountable for the enhanced hair density in DMN-VPA-treated mice.

We found that dermal thickness was more variable and higher in mice that had received the DMN control than in topical control-treated mice. The correlation of micro-wounding with upregulation of Wnt/ β-catenin pathway may explain this phenomenon. In addition, activation of epidermal Wnt/ β-catenin signaling plays an important role in thickness of adipocyte tissue which is also known to regulate HF growth [56]. Therefore, we speculate that a longer experimental period might reveal earlier anagen onset in DMN control- than in topical control-treated mice. Furthermore, as the effects of DMN-VPA application may differ based on the hair cycle phase in which VPA is applied, we suggest this potential correlation should be researched in future studies.

While our findings suggest the potential of micro-wounding for HF regrowth, there remains a need for future detailed studies on the effects of micro-wounding depth, distance between micro-wounds, and extended animal tests focusing on micro-wounding. The micro-wound dimension is correlated with the geometry of DMN-VPA; therefore, we assume that different geometries alter the extent to which HF-inducing proteins and pathways are upregulated. Based on our *in vivo* findings, we assume that through optimization of the micro-wounds and VPA dose, it is possible to enhance the efficiency of DMN-VPA even further. Moreover,

addition of platelet-rich plasma (PRP), an autologous blood product of a patient, to the solution of VPA may effectively improve the hair growth capability of DMNs [57]. Additional investigation on the synergic effects of VPA combined with PRP-DMNs is remained to be performed in further studies. In this study, we found that DMN-VPA promotes hair regrowth more effectively than topical VPA, whereas in our future research, we will perform detailed analysis on hair generation at each growth phase using specific animal models.

5. Conclusion

Our findings indicate that implantation of the dual-functionalized micro-wound mediated DMN-VPA system can be utilized as a potential candidate for inducing hair regrowth with a significantly improved efficiency, accuracy, and effectiveness compared with the current, commonly used androgenetic alopecia-treating systems.

Acknowledgements

We thank Geonwoo Kim and professor Samuel Carroll Brooks III for helpful discussions and their support throughout the research. This work was supported and funded equally by a grant from the National Research Foundation (NRF), the Translational Research Center for Protein Function Control (Grant No.2016R1A5A1004694) and a grant from the Korea Health Technology R&D Project through the Korea Health Industry Development Institute (KHIDI), funded by the Ministry of Health & Welfare, Republic of Korea (grant number: HI16C0625 and HI14C0365).

Conflict of interest: The authors state no conflict of interest.

Data availability: The raw/processed data required to reproduce these findings cannot be shared at this time as the data also forms part of an ongoing study.

References

[1] T. Ito, Advances in the management of alopecia areata, J. Dermatol. 39 (2012) 11-17.
[2] L. Petukhova, M. Duvic, M. Hordinsky, D. Norris, V. Price, Y. Shimomura, H. Kim, P. Singh, A. Lee, W.V. Chen, K.C. Meyer, R. Paus, C.A. Jahoda, C.I. Amos, P.K. Gregersen, A.M. Christiano, Genome-wide association study in alopecia areata implicates both innate and adaptive immunity, Nature. 466 (2010) 113-117.
[3] L. Xing, Z. Dai, A. Jabbari, J.E. Cerise, C.A. Higgins, W. Gong, A. de Jong, S. Harel, G.M. DeStefano, L. Rothman, P. Singh, L. Petukhova, J. Mackay-Wiggan, A.M. Christiano, R. Clynes, Alopecia areata is driven by cytotoxic T lymphocytes and is reversed by JAK inhibition, Nat. Med. 20 (2014) 1043-1049.
[4] R.P. Dawber, J. Rundegren, Hypertrichosis in females applying minoxidil topical solution and in normal controls, J. Eur. Acad. Dermatol. Venereol. 17 (2003) 271-275.
[5] M. Gonzalez, N. Landa, J. Gardeazabal, M.J. Calderon, I. Bilbao, J.L. Diaz Perez, Generalized hypertrichosis after treatment with topical minoxidil, Clin. Exp. Dermatol. 19 (1994) 157-158.
[6] A.R. MacMillan, F.J. Warshawski, R.A. Steinberg, Minoxidil overdose, Chest. 103 (1993) 1290-1291.
[7] A.V. D'Amico, C.G. Roehrborn, Effect of 1 mg/day finasteride on concentrations of serum prostate-specific antigen in men with androgenic alopecia: a randomised controlled trial, Lancet. Oncol. 8 (2007) 21-25.
[8] J.S. Crabtree, E.J. Kilbourne, B.J. Peano, S. Chippari, T. Kenney, C. McNally, W. Wang, H.A. Harris, R.C. Winneker, S. Nagpal, C.C. Thompson, A mouse model of androgenetic alopecia, Endocrinology. 151 (2010) 2373-2380.
[9] M.K. Samplaski, A.K. Nangia, Adverse effects of common medications on male fertility, Nat. Rev. Urol. 12 (2015) 401-413.
[10] C.U. Johannessen, Mechanisms of action of valproate: a commentatory, Neurochem. Int. 37 (2000) 103-110.
[11] E. Perucca, Pharmacological and therapeutic properties of valproate: a summary after 35 years of clinical experience, CNS Drugs. 16 (2002) 695-714.
[12] S.J. Jo, H. Shin, Y.W. Park, S.H. Paik, W.S. Park, Y.S. Jeong, H.J. Shin, O. Kwon, Topical valproic acid increases the hair count in male patients with androgenetic alopecia: a randomized, comparative, clinical feasibility study using phototrichogram analysis, J. Dermatol. 41 (2014) 285-291.
[13] S.Y. Choi, H.D. Kim, B.J. Kim, M.N. Kim, D.H. Han, A case of androgenetic alopecia treated with valproic acid, Int. J. Dermatol. 53 (2014) e214-215.
[14] S.J. Jo, S.J. Choi, S.Y. Yoon, J.Y. Lee, W.S. Park, P.J. Park, K.H. Kim, H.C. Eun, O. Kwon, Valproic acid promotes human hair growth in in vitro culture model, J. Dermatol. Sci. 72 (2013) 16-24.
[15] M.F. Reynolds, E.C. Sisk, N.L. Rasgon, Valproate and neuroendocrine changes in relation to women treated for epilepsy and bipolar disorder: a review, Curr. Med. Chem. 14 (2007) 2799-2812.
[16] S.H. Lee, M. Zahoor, J.K. Hwang, S. Min do, K.Y. Choi, Valproic acid induces cutaneous wound healing in vivo and enhances keratinocyte motility, PLoS One. 7 (2012) e48791.

[17] S.H. Lee, J. Yoon, S.H. Shin, M. Zahoor, H.J. Kim, P.J. Park, W.S. Park, S. Min do, H.Y. Kim, K.Y. Choi, Valproic acid induces hair regeneration in murine model and activates alkaline phosphatase activity in human dermal papilla cells, PLoS One. 7 (2012) e34152.
[18] J. Wiltse, Mode of action: inhibition of histone deacetylase, altering WNT-dependent gene expression, and regulation of beta-catenin--developmental effects of valproic acid, Crit. Rev. Toxicol. 35 (2005) 727-738.
[19] J. Huelsken, R. Vogel, B. Erdmann, G. Cotsarelis, W. Birchmeier, beta-Catenin controls hair follicle morphogenesis and stem cell differentiation in the skin, Cell. 105 (2001) 533-545.
[20] S.H. Yang, T. Andl, V. Grachtchouk, A. Wang, J. Liu, L.J. Syu, J. Ferris, T.S. Wang, A.B. Glick, S.E. Millar, A.A. Dlugosz, Pathological responses to oncogenic Hedgehog signaling in skin are dependent on canonical Wnt/beta3-catenin signaling, Nat. Genet. 40 (2008) 1130-1135.
[21] W.H. Lien, L. Polak, M. Lin, K. Lay, D. Zheng, E. Fuchs, In vivo transcriptional governance of hair follicle stem cells by canonical Wnt regulators, Nat. Cell. Biol. 16 (2014) 179-190.
[22] S.E. Millar, Molecular mechanisms regulating hair follicle development, J. Invest. Dermatol. 118 (2002) 216-225.
[23] J.W. Oh, J. Kloepper, E.A. Langan, Y. Kim, J. Yeo, M.J. Kim, T.C. Hsi, C. Rose, G.S. Yoon, S.J. Lee, J. Seykora, J.C. Kim, Y.K. Sung, M. Kim, R. Paus, M.V. Plikus, A Guide to Studying Human Hair Follicle Cycling In Vivo, J. Invest. Dermatol. 136 (2016) 34-44.
[24] R. Paus, G. Cotsarelis, The biology of hair follicles, N. Engl. J. Med. 341 (1999) 491-497.
[25] S.H. Lee, M.Y. Kim, H.Y. Kim, Y.M. Lee, H. Kim, K.A. Nam, M.R. Roh, S. Min do, K.Y. Chung, K.Y. Choi, The Dishevelled-binding protein CXXC5 negatively regulates cutaneous wound healing, J. Exp. Med. 212 (2015) 1061-1080.
[26] H.S. Go, K.C. Kim, C.S. Choi, S.J. Jeon, K.J. Kwon, S.H. Han, J. Lee, J.H. Cheong, J.H. Ryu, C.H. Kim, K.H. Ko, C.Y. Shin, Prenatal exposure to valproic acid increases the neural progenitor cell pool and induces macrocephaly in rat brain via a mechanism involving the GSK-3beta/beta-catenin pathway, Neuropharmacology. 63 (2012) 1028-1041.
[27] G.A. Jung, J.Y. Yoon, B.S. Moon, D.H. Yang, H.Y. Kim, S.H. Lee, V. Bryja, E. Arenas, K.Y. Choi, Valproic acid induces differentiation and inhibition of proliferation in neural progenitor cells via the beta-catenin-Ras-ERK-p21Cip/WAF1 pathway, BMC Cell Biol. 9 (2008) 66.
[28] G.E. Rogers, P.I. Hynd, Animal models and culture methods in the study of hair growth, Clin. Dermatol. 19 (2001) 105-119.
[29] F.H. Gage, Mammalian neural stem cells, Science, 287 (2000) 1433-1438.
[30] M. Kahn, Can we safely target the WNT pathway?, Nat. Rev. Drug Discov. 13 (2014) 513-532.
[31] P. Cohen, M. Goedert, GSK3 inhibitors: development and therapeutic potential, Nat. Rev. Drug Discov. 3 (2004) 479-487.
[32] S. Yasuda, M.H. Liang, Z. Marinova, A. Yahyavi, D.M. Chuang, The mood stabilizers lithium and valproate selectively activate the promoter IV of brain-derived neurotrophic factor in neurons, Mol. Psychiatry. 14 (2009) 51-59.
[33] R. Guerrini, Valproate as a mainstay of therapy for pediatric epilepsy, Paediatr. Drugs. 8 (2006) 113-129.
[34] M. Servadio, F. Melancia, A. Manduca, A. di Masi, S. Schiavi, V. Cartocci, V. Pallottini, P. Campolongo, P. Ascenzi, V. Trezza, Targeting anandamide metabolism rescues core and

associated autistic-like symptoms in rats prenatally exposed to valproic acid, Transl. Psychiatry. 6 (2016) e902.
[35] M. Dangol, H. Yang, C.G. Li, S.F. Lahiji, S. Kim, Y. Ma, H. Jung, Innovative polymeric system (IPS) for solvent-free lipophilic drug transdermal delivery via dissolving microneedles, J. Control. Release. 223 (2016) 118-125.
[36] E. Fuchs, Scratching the surface of skin development, Nature. 445 (2007) 834-842.
[37] S.P. Sullivan, D.G. Koutsonanos, M. Del Pilar Martin, J.W. Lee, V. Zarnitsyn, S.O. Choi, N. Murthy, R.W. Compans, I. Skountzou, M.R. Prausnitz, Dissolving polymer microneedle patches for influenza vaccination, Nat. Med. 16 (2010) 915-920.
[38] S. Hirobe, H. Azukizawa, T. Hanafusa, K. Matsuo, Y.S. Quan, F. Kamiyama, I. Katayama, N. Okada, S. Nakagawa, Clinical study and stability assessment of a novel transcutaneous influenza vaccination using a dissolving microneedle patch, Biomaterials. 57 (2015) 50-58.
[39] P.S. Myung, M. Takeo, M. Ito, R.P. Atit, Epithelial Wnt ligand secretion is required for adult hair follicle growth and regeneration, J. Invest. Dermatol. 133 (2013) 31-41.
[40] S. Cheon, R. Poon, C. Yu, M. Khoury, R. Shenker, J. Fish, B.A. Alman, Prolonged beta-catenin stabilization and tcf-dependent transcriptional activation in hyperplastic cutaneous wounds, Lab. Invest. 85 (2005) 416-425.
[41] R. Sumagin, J.C. Brazil, P. Nava, H. Nishio, A. Alam, A.C. Luissint, D.A. Weber, A.S. Neish, A. Nusrat, C.A. Parkos, Neutrophil interactions with epithelial-expressed ICAM-1 enhances intestinal mucosal wound healing, Mucosal. Immunol. 9 (2016) 1151-1162.
[42] M. Ito, Z. Yang, T. Andl, C. Cui, N. Kim, S.E. Millar, G. Cotsarelis, Wnt-dependent de novo hair follicle regeneration in adult mouse skin after wounding, Nature. 447 (2007) 316-320.
[43] M.B. Labus, C.M. Stirk, W.D. Thompson, W.T. Melvin, Expression of Wnt genes in early wound healing, Wound Repair Regen. 6 (1998) 58-64.
[44] D.L. Zhang, L.J. Gu, L. Liu, C.Y. Wang, B.S. Sun, Z. Li, C.K. Sung, Effect of Wnt signaling pathway on wound healing, Biochem. Biophys. Res. Commun. 378 (2009) 149-151.
[45] R.E. Billingham, P.S. Russell, Incomplete wound contracture and the phenomenon of hair neogenesis in rabbits' skin, Nature. 177 (1956) 791-792.
[46] A.M. Kligman, J.S. Strauss, The formation of vellus hair follicles from human adult epidermis, J. Invest. Dermatol. 27 (1956) 19-23.
[47] S.F. Lahiji, M. Dangol, H. Jung, A patchless dissolving microneedle delivery system enabling rapid and efficient transdermal drug delivery, Sci. Rep. 5 (2015) 7914.
[48] H. Yang, S. Kim, G. Kang, S.F. Lahiji, M. Jang, Y.M. Kim, J.M. Kim, S.N. Cho, H. Jung, Centrifugal Lithography: Self-Shaping of Polymer Microstructures Encapsulating Biopharmaceutics by Centrifuging Polymer Drops, Adv Healthc Mater 6(19) (2017).
[49] M. Drosten, C.G. Lechuga, M. Barbacid, Ras signaling is essential for skin development, Oncogene. 33 (2014) 2857-2865.
[50] H. Alam, L. Sehgal, S.T. Kundu, S.N. Dalal, M.M. Vaidya, Novel function of keratins 5 and 14 in proliferation and differentiation of stratified epithelial cells, Mol. Biol. Cell. 22 (2011) 4068-4078.
[51] G. Solanas, S.A. Benitah, Regenerating the skin: a task for the heterogeneous stem cell pool and surrounding niche, Nat. Rev. Mol. Cell. Biol. 14 (2013) 737-748.
[52] K.E. Toyoshima, K. Asakawa, N. Ishibashi, H. Toki, M. Ogawa, T. Hasegawa, T. Irie, T. Tachikawa, A. Sato, A. Takeda, T. Tsuji, Fully functional hair follicle regeneration through the rearrangement of stem cells and their niches, Nat. Commun. 3 (2012) 784.

[53] I. Huh, S. Kim, H. Yang, M. Jang, G. Kang, H. Jung, Effects of two droplet-based dissolving microneedle manufacturing methods on the activity of encapsulated epidermal growth factor and ascorbic acid, Eur J Pharm Sci 114 (2018) 285-292.
[54] G. Cotsarelis, T.T. Sun, R.M. Lavker, Label-retaining cells reside in the bulge area of pilosebaceous unit: implications for follicular stem cells, hair cycle, and skin carcinogenesis, Cell. 61 (1990) 1329-1337.
[55] D. Gay, O. Kwon, Z. Zhang, M. Spata, M.V. Plikus, P.D. Holler, M. Ito, Z. Yang, E. Treffeisen, C.D. Kim, A. Nace, X. Zhang, S. Baratono, F. Wang, D.M. Ornitz, S.E. Millar, G. Cotsarelis, Fgf9 from dermal gammadelta T cells induces hair follicle neogenesis after wounding, Nat. Med. 19 (2013) 916-923.
[56] G. Donati, V. Proserpio, B.M. Lichtenberger, K. Natsuga, R. Sinclair, H. Fujiwara, F.M. Watt, Epidermal Wnt/beta-catenin signaling regulates adipocyte differentiation via secretion of adipogenic factors, Proc. Natl. Acad. Sci. U. S. A. 111 (2014) E1501-1509.
[57] S. Giordano, M. Romeo, P. Lankinen, Platelet-rich plasma for androgenetic alopecia: Does it work? Evidence from meta analysis, J Cosmet Dermatol 16(3) (2017) 374-381.